The Speed Prediction Research of Peak Particle Vibration Velocity in Underwater Blasting Based on GWO-SVR

Juntao Sun
Yunnan Institute of Water and Hydropower Engineering Investigation, Design and Research
Jingzhu Huang
690488311@163.com

School of Civil and Surveying Engineering, Jiangxi University of Science and Technology
Zhiwei He
Guangzhou Pearl River Supervision and Consulting Group Co., LTD
Jiahe Wang
Gaoke Landscape Co.,Lto, Xi"an
Dawei Zhan
Hunan Huachu Project Management Co., Ltd
Qingxiong Zhu
Yunnan Water Conservancy and Hydropower Engineering Co., Ltd

Research Article

Keywords: underwater blasting, GWO-SVR, PPV, artificial intelligence

Posted Date: February 23rd, 2024

DOI: https://doi.org/10.21203/rs.3.rs-3971503/v1

Additional Declarations: Competing interest reported. Conflict of interest I declare that there is no confict of in terest.

The Speed Prediction Research of Peak Particle Vibration Velocity in Underwater Blasting Based on GWO-SVR

Juntao Sun [1,2], Jingzhu Huang [2*], Zhiwei He [3], Jiahe Wang [4], Dawei Zhan [5], Qingxiong Zhu [6]

(1. Yunnan Institute of Water and Hydropower Engineering Investigation, Design and Research, Kunming 650021, Yunnan China; 2. School of Civil and Surveying Engineering, Jiangxi University of Science and Technology, Ganzhou 341000, Jiangxi, China; 3. Guangzhou Pearl River Supervision and Consulting Group Co., LTD, 4. Gaoke Landscape Co.,Lto, Xi"an, Xian 710075, Shaanxi China; 5. Hunan Huachu Project Management Co., Ltd, Changsha 410007, Hunan China; 6. Yunnan Water Conservancy and Hydropower Engineering Co., Ltd, Kunming , 650500 Yunnan China)

Corresponding author(s). E-mail(s): 690488311@163.com

Abstract: The blasting vibration produced in the blasting process of underwater engineering brings serious damage to the surrounding environment. Predicting blasting peak particle velocity (PPV) is one of the effective ways to alleviate the problem. To further improve the prediction accuracy of blast PPV, the grey wolf optimization (GWO) algorithm is used in this paper to optimize the penalty factor and radial basis kernel function parameters of support vector regression (SVR) model iteratively, and a blasting PPV prediction model was established. Taking the Dajin Island water intake open channel of the Phase 1 project of Guangdong Taishan Nuclear Power Station as the engineering background, according to the relevant parameters of blasting vibration recorded in 30 blasting tests, taking into account blasting design parameters and geological conditions, a database consisting of 12 inputs (hole length (*HL*), spacing (*S*), row spacing (R_s), burden (*B*), stemming length (l_s), the distance of blasting center (B_d), height differential elevation (H_{de}), seawater pressure (P_s), powder factor (*PF*), maximum charge of single hole (Q_{smax}), maximum charge per delay (Q_{max}) and total charge (Q_{tot}) and 1 output (PPV)) was established. Then, the grey wolf optimization-support vector regression (GWO-SVR) model, double-layer neural network, medium decision tree, and empirical SVR model are used to establish a prediction model for the PPV in underwater blasting respectively, and the prediction results are compared and analyzed. The results are as follows: the actual value - predicted value diagram and residual comparison show that the prediction effect of PPV based on the double layer neural network model is the worst in underwater blasting. The comparison of regression evaluation indexes shows that GWO-SVR is the best method for predicting PPV in underwater blasting; its R^2 is 0.9285, *RMSE* is 0.21424, *MSE* is 0.0459 and *MAE* is 0.1625. The research results can provide a theoretical reference for the construction of similar underwater blasting projects, and provide a scientific basis for delineating a reasonable safety warning range for similar underwater blasting projects.

Key words: underwater blasting; GWO-SVR; PPV; artificial intelligence

Introduction

Underwater blasting is the main construction method for underwater earthwork excavation such as water resources and hydropower engineering, Port and wharf construction, bridge engineering and dam construction. Compared with land blasting, underwater engineering blasting is not only difficult to construct and requires high technology, but also more serious to the surrounding environment. Accurately analyzing and predicting the law of peak particle velocity (PPV) caused by blasting and then optimizing blasting design and construction is one of the effective methods to effectively reduce blasting vibration hazards (Verma et al 2018; Zhang et al 2019; Li et al 2019). Therefore, many scholars at home and abroad conducted a great deal of research on blast vibration velocity prediction, and achieved many rich results.

In the age of undeveloped technology last century, the general method for predicting the PPV is: taking into account the relationship between the blasting design parameters and the PPV, and establish a corresponding empirical expression, such as the Sadowski's formula considering the amount of charge and the distance from the blast source (Wang et al 2020; Lu et al 2011; Zhang et al 2020); there are also some theoretical expressions established based on the propagation law of stress waves (Duvall and Fogelson 1962; Zhang et al 2021; Wang et al 2017); but the above empirical and theoretical formulas can only consider 2 ~ 3 factors at the same time, in fact, the influence factors of the PPV is very much, such as the hole length (HL), spacing (S), row spacing (R_s), burden (B), stemming length (l_s), the distance of blasting center (B_d), powder factor (PF), maximum charge of single hole (Q_{smax}), maximum charge per delay (Q_{max}) and total charge (Q_{tot}), etc, so the prediction result is not consistent with actual situation. With the development of computers, numerical simulation computing technology has been widely applied to blasting engineering (Hao et al 2002; Saiang and Nordlund 2009; Wang et al 2020), but the numerical values need to simplify boundary conditions and material properties, so the obtained results are different from the actual situation. Given that machine learning can take into account multiple blasting factors, artificial intelligence is also widely used in the blasting field. For example, the PPV prediction model established by neural network (Nguyen et al 2019; Shang et al 2019; Taheri et al 2017; Yang et al 2019), decision tree (Khandelwal et al 2017; Rana et al 2020; Bhagat et al 2022), support vector regression (SVR) (Hasanipanah et al 2015; Khandelwal 2011; Shi et al 2012; Yang et al 2019), etc.

However, the construction of models based on artificial neural network or decision tree for predicting the PPV lead to problems such as over-fitting of the datas (Paneiro et al 2018; Lawal and Idris 2020; Hasanipanah et al 2017; Nguyen et al 2019). Although SVR has good generalization performance and is not easy to overfit, the choice of penalty factor c and kernel function parameter g has a critical impact on the prediction accuracy of the model when it is used to predict PPV. Moreover, there is no systematic guiding principle or method for the selection of c and g at present, and most of them are based on experiences and trial-and-error methods (Abdi and Giveki 2013; Hasanipanah et al 2017; Armaghani et al 2020; Murillo-Escobar et al 2019;). In addition, during underwater blasting, blasting vibration velocity is not only related to blasting design parameters, but also to the geological conditions of the blasting sites, such as water pressure, height differential elevation due to topographies (Khandelwal and Singh 2009; Khandelwal 2011; Hajihassani et al 2015 a, b).

Therefore, based on the engineering background of the Dajin Island water intake open channel of the Phase 1 project of Guangdong Taishan Nuclear Power Station, this paper establishes a PPV prediction model based on grey wolf optimization-support vector regression (GWO-SVR) (Balogun et al 2022), considering various blasting design parameters, water pressure, and height differential evlevation caused by topography and geomorphology. The algorithm chooses the SVR as the base model and builds an optimisation model based on finding the best initial parameters that conform to the actual engineering. Then the PPV of the blasting is predicted based on the optimization model, and the prediction results are compared with the double-layer neural network, medium decision tree, and empirical SVR model to test the rationality and feasibility of the model. The research results can provide a theoretical reference for similar underwater blasting construction.

Engineering background

The Guangdong Taishan Nuclear Power Station is located in Yaogu Village, Chixi Town, Taishan City, Jiangmen, with the Huangmao Sea to the east of the plant site and Dajin Island about 5km to the southeast (as shown in Figure 1). The construction scale of the project is 6×1750MW (EPR), which is divided into three phases. In the first phase of the Dajin Island water intake open channel, dredging in the 0+90~0+200 m mileage section of the canal requires underwater reef blasting construction (Zeng et al 2016), and the construction volume is about 203407.1m^3. The bedrocks in this area are mainly sandstone and mudstone, and the main mineral components are quartz and feldspar. The bedding, joint and fissure of the rock layers are well developed, and the coverings include gravel, pebble and silt, etc. In order to ensure that the vibration velocity of the newly poured concrete dam gate of the 1$^\#$~2$^\#$ shafts of the water intake tunnel does not exceed the safety threshold during the blasting excavation process, it is necessary to accurately predict the blasting excavation of the underwater rock.

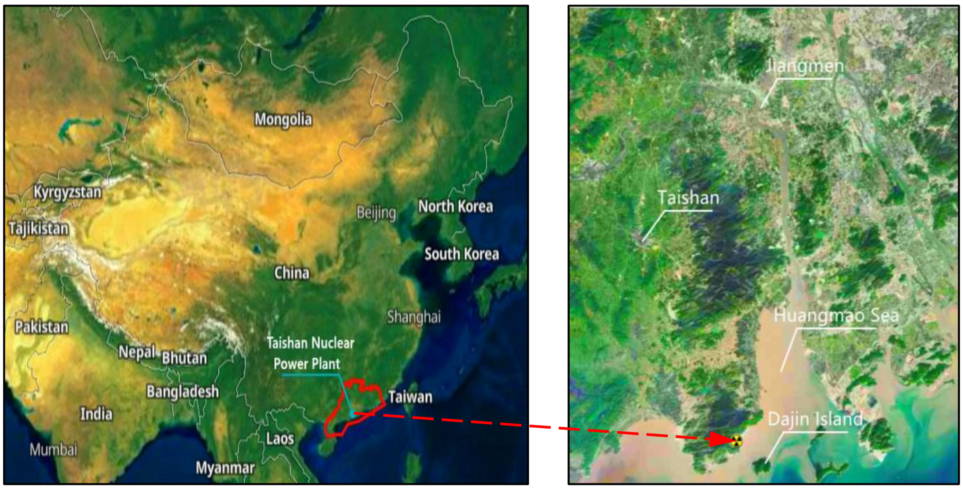

Figure. 1. Distribution of Taishan Nuclear Power Plant in Guangdong province

Thirty blasting tests were carried out prior to the large scale underwater blasting excavation, with 115 mm diameter holes and basically the same charging pattern, all detonated in sections, with the same type of emulsion explosive. The charging structure of underwater blasting and the layout of on-site vibration monitoring points are shown in Figure 2, and the monitoring results are shown in Table 1 (Liu et al 2013). The following 12 variables were selected on this occasion as the main factors that may affect the blast vibration velocity: hole length (*HL*), spacing (*S*), row spacing (R_s), burden (*B*), stemming length (l_s), the distance of blasting center (B_d), height differential elevation (H_{de}), seawater pressure (P_s), powder factor (*PF*), maximum charge of single hole (Q_{smax}), maximum charge per delay (Q_{max}) and total charge (Q_{tot}).

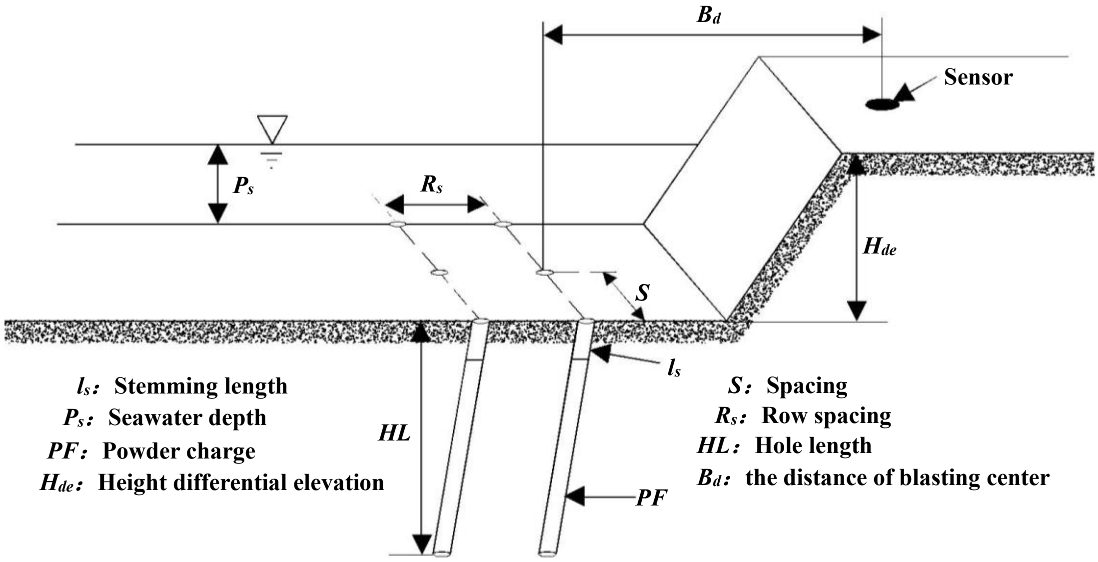

Figure 2. Layout of the blasting charge and site monitoring of underwater blasting

Table 1. Site monitoring results on underwater blasting (Liu et al 2013)

N	*HL* /m	*S*/m	R_s/m	*B*/m	l_s/m	B_d/m	H_{de}/m	P_s/(10 kPa)	*PF*/kg	Q_{smax}/kg	Q_{max}/kg	Q_{tot}/kg	*PPV*/(cm/s)
1	7.8	3.0	3.0	4.0	1.9	97.4	35.7	7.7	1.2	54	80	960	2.010
2	7.9	3.0	3.0	4.0	1.9	136.7	35.4	7.4	1.3	50	78	1200	1.150
3	8.3	3.0	3.0	4.0	2.0	167.6	34.9	7.0	1.1	40	62	960	0.714
4	5.0	3.5	3.0	4.5	1.8	191.7	38.8	10.7	1.2	16.8	52	312	0.631
5	9.5	3.0	3.0	4.0	2.0	108.1	34.3	6.4	1.2	40	80	960	2.350
6	7.8	3.5	3.0	4.5	1.8	194.6	37.4	9.3	1.3	27	54	648	0.610
7	9.5	3.5	3.5	4.5	2.2	161.5	34.1	6.4	1.1	40	160	960	1.170
8	8.3	3.5	3.5	4.0	2.0	140.7	34.1	6.2	1.1	37	150	888	1.330
9	8.2	3.5	3.5	4.0	2.0	130.9	34.2	6.3	1.1	30	130	792	0.491
10	9.1	3.0	3.0	4.0	2.0	132.0	34.2	6.3	1.3	62	50	1200	0.553
11	10.3	3.0	3.0	4.0	2.4	153.9	32.6	5.1	1.2	49	80	960	0.783
12	8.6	3.0	3.0	4.0	2.0	155.5	34.5	6.6	1.2	40	80	960	0.694

Continuation of table 1

N	HL /m	S/m	R_s/m	B/m	l_s/m	B_d/m	H_{de}/m	P_s/(10 kPa)	PF/kg	Q_{smax}/kg	Q_{max}/kg	Q_{tol}/kg	PPV/(cm/s)
13	9.1	3.0	3.0	4.0	2.0	116.4	34.0	6.1	1.2	38	65	960	0.670
14	10.4	3.0	3.0	4.0	2.5	110.8	32.8	5.4	1.2	37	50	960	0.444
15	10.1	3.0	3.0	4.0	2.4	199.6	32.8	5.3	1.1	40	55	960	0.843
16	10.7	3.0	3.0	4.0	2.5	103.2	32.7	5.3	1.2	51	78	960	1.080
17	10.6	3.0	3.0	4.0	2.5	97.8	32.6	5.2	1.2	40	80	960	1.930
18	9.5	3.0	3.0	4.0	2.2	173.4	33.7	6.0	1.2	39	78	960	1.150
19	9.3	3.0	3.0	4.0	2.2	158.2	33.7	6.0	1.2	35	70	960	0.699
20	6.5	3.0	3.0	4.0	1.6	135.2	36.9	8.6	1.3	67	75	1200	1.030
21	7.9	3.0	3.0	4.0	1.9	132.2	35.4	7.4	1.1	40	80	960	1.130
22	8.9	3.0	3.0	4.0	2.0	98.7	34.8	6.9	1.2	40	80	960	2.200
23	11.1	3.0	3.0	4.0	2.5	158.6	32.0	4.6	1.2	39	68	960	1.020
24	7.0	3.5	3.0	4.5	1.8	195.3	38.9	10.8	1.2	25	50	600	0.357
25	9.8	3.0	3.0	4.0	2.2	106.5	33.3	5.6	1.2	40	70	960	1.156
26	8.1	3.0	3.0	4.0	1.9	130.6	35.1	7.1	1.1	53	48	960	0.588
27	10.5	3.0	3.0	4.0	2.4	162.2	32.6	5.1	1.2	54	80	960	1.560
28	11.1	3.0	3.0	4.0	2.5	182.5	31.9	4.5	1.1	48	53	960	0.724
29	6.2	3.0	3.0	4.0	1.6	135.8	37.2	8.9	1.3	48	75	1200	0.821
30	6.0	3.5	3.5	4.0	1.6	191.7	39.4	11.2	1.2	48	120	720	0.476

Gwo-svr model and application

Support vector regression (SVR)

Support Vector Regression (SVR) is an application of Support Vector Machine (SVM) to regression problems (Smola and Schölkopf 2004; Mahmoodzadeh et al 2021).

The principle is: a "spacer band" is created on both sides of the linear function, and no loss is calculated for all samples that fall within the interval band; Only samples outside the interval band are counted in the loss function. The model is then optimized by minimizing the width of the spacer and the total loss.

For a given training sample D={(x_1,y_1), (x_2,y_2),…, (x_n,y_n)}, $y_i \in$R, we want to learn an *f(x)* that is as close as possible to *y*; *w, b* are the parameters to be determined. In this model, the loss is zero only if *f(x)* is the same as *y*; the SVR assumes that the maximum allowable deviation between *f(x)* and *y* is ε, loss is calculated if and only if the absolute value of the difference between *f(x)* and *y* is greater than ε, at this time, it is equivalent to constructing an interval with a width of 2ε with *f(x)* as the center. If the training sample falls into this interval, it is considered to be correctly predicted. (The amount of slack on both sides of the spacer can vary)

Cortes and Vapnik (Cortes and Vapnik 1995) used an error function known as the -insensitive error function, giving the SVM the following regression form:

$$L(y, f(x,\alpha)) = |y - f(x,\alpha)|_{\varepsilon} = \begin{cases} 0 & \text{if } |y - f(x,\alpha)| \le \varepsilon \\ |y - f(x,\alpha)| - \varepsilon & \text{otherwise} \end{cases} \tag{1}$$

In equation (1), the error of less than is ignored. In other words, errors in the range of less than are not penalized by this function. This range is called a tubular insensitive region and has the form of a plate in multidimensional problems, or the range lies between two parallel hyperplanes. In order to develop an algorithm, the estimation of a linear function should first be evaluated. All linear functions have the following general form.

$$f(x) = \langle w, x \rangle + b, w, x \in X, b \in R \tag{2}$$

where <, .> denotes the inner product of two vectors in Hilbert space (*w* is the weight vector and *x* is the input space). The goal of the learning trend is to determine a function $\subseteq X*Y$ with minimum error and uniform distribution of (x_1, y_1),…,(x_m, y_m) based on independent data, called the -SVR algorithm. To this end, an attempt is made to minimize the generalized error function R_{reg} based on the -insensitive error function. R_{reg} can be rewritten based on the extended form of R_{emp}, so

$$R^{\varepsilon}_{\text{emp}}[f] = \frac{1}{m}\sum_{i=1}^{m} |y_i - f(x_i)|_{\varepsilon} \; [f = \frac{1}{2}\|w\|^{2C} + C.R^{\varepsilon}_{emp}[f]] \tag{3}$$

where R_{emp} calculates the training error in the insensitive error function and *C* is a constant that somehow determines the value of $\|w\|^2$ given the complexity of the function. The minimizing equation (3) shows that the main idea of statistical learning theory is to achieve a true minimum error, thus requiring control over the model complexity as well as the error corresponding to the training data (Cortes and Vapnik 1995). After solving the above optimization problem, the values of *f* and *w*, respectively, are obtained as follows:

$$w = \sum_{i=1}^{m} (a_i^* - a_i) x_i$$
$$f(x) = \sum_{i=1}^{m} (a_i^* - a_i) \langle x_i, x \rangle + b \tag{4}$$

A kernel function is a vector product of functions, in which data is passed through the function to a higher dimensional space. Various kernel functions can be used, such as linear kernel, radial kernel, polynomial kernel, and sigmoid kernel. Therefore, in nonlinear problems, it is sufficient to use a kernel of the input values rather than the function itself. Considering the theory explained, the parameter values and parameter values present in the kernel function have a significant impact on the error reduction of the problem when determining the smoothing parameter *C*.

Grey wolf optimization algorithm

Creatures under the harsh environment of nature, even if they do not possess the high intelligence of human beings, they have shown amazing group intelligence through continuous adaptation and collective cooperation under the same goal, that is, motivated by food. By observing the strict organizational system of wolves and their exquisite cooperative hunting methods (Emary et al 2016), scholars such as Mirjalili (Mirjalili et al 2014) in Australia proposed a new swarm intelligence algorithm-grey wolf optimization algorithm.

The gray wolf population has a strict hierarchical system, which is similar to a kind of pyramid. The head wolf at the top of the pyramid is called *α*, and its responsibility is to make decisions about hunting behavior, habitat, food distribution, etc.

The principle is as follows: There are three wolves *α*, *β*, and *δ* in the gray wolf population as the head wolf, of which *α* is the wolf king, located at the top of the pyramid, and is mainly responsible for leading the entire gray wolf group; *β* is located on the second level of the pyramid, when the entire wolf pack is missing *α*, *β* takes over from *α* wolf, giving orders; *δ* is located on the third level of the pyramid and follow the orders of the *α* and *β* wolves. The bottom layer is *ω* wolf, obey the command of the upper three layers.

The process of wolves looking for prey is the process of finding the optimal solution. The process includes the steps of population initialization, social hierarchy stratification, encirclement, hunting, attacking prey and finding prey. The mathematical model of the algorithm is as follows:

(1) Population initialization: All individual wolves are randomly distributed into the search domain, namely:

$$X_i(1,2,\ldots, M) \sim R(lb,ub) \tag{5}$$

In the formula: X_i is the individual gray wolf; *n* is the number of gray wolf individuals, that is, the population; *M* is the population dimension; *lb* and *ub* are the upper and lower boundaries of the search area; *R* is a random distribution function.

(2) Social class stratification: Fitness values are calculated for all individual wolves, and label the three gray wolves with the best fitness as *α*, *β*, *δ*, and the remaining gray wolves as *ω*. *α(a)* as the optimal solution, *β(b)* and *δ(d)* as the suboptimal solutions, and the remaining candidate solutions are *ω(x)*. The hunting in the gray wolf algorithm is led by *α*, *β*, *δ*, and *ω* searches for the prey under the guidance of these three wolves (optimal solution).

(3) Surrounding the prey: The mathematical model of a grey wolf gradually approaching its prey and surrounding it. Its mathematical model is as follows (Mirjalili et al 2014):

$$D = \left| C \cdot X_p(t) - X(t) \right| \tag{6}$$

$$X(t+1) = X_P - A \cdot D \tag{7}$$

$$a = 2 - \frac{2t}{\max t} \tag{8}$$

$$A = 2a \cdot r_1 - a \tag{9}$$

$$C = 2r_2 \tag{10}$$

where: t indicates the number of steps in the current iteration; max t represents the maximum number of iteration steps; "." represents the Hadamard product operation; A and C are synergy coefficients; $\boldsymbol{D}$ is the distance between wolf and prey; $\boldsymbol{X}_\mathrm{p}$ is the prey position; $\boldsymbol{X}$(t) indicates the current position of the grey wolf; In the whole iterative process, the convergence factor a decreases linearly from 2 to 0; r_1 and r_2 are random numbers in [0,1].

(4) Hunting: Keep the best three gray wolves (α, β, δ) in the population at each iteration, then in the next iteration, update the positions of all wolves according to their position information. The mathematical model for this behavior is as follows:

$$D_k = \left| C_k \cdot X_k(t) - X(t) \right| \tag{11}$$

$$X_i(t+1) = X_k(t) - E \cdot D_i \tag{12}$$

$$X(t+1) = \frac{X_1 + X_2 + X_3}{3} \tag{13}$$

In the formula: $k = \alpha, \beta, \delta$, i = 1, 2, 3; $\boldsymbol{X}_\alpha$, $\boldsymbol{X}_\beta$, $\boldsymbol{X}_\gamma$ represent the optimal three wolf positions in the current population, respectively; $\boldsymbol{X}$ indicates the position vector of other candidate wolves; D_α, D_β, D_γ denote the distance between the current candidate grey wolf and the optimal three wolves respectively.

(5) Attacking the prey: Building a prey model for attack. $\boldsymbol{E}$ is a random vector in the interval [-a,a], when a=1, $\boldsymbol{E}$ belongs to [-1,1].

(6) Finding the prey: When $|\boldsymbol{B}|>1$, all gray wolves are scattered in various areas to search for prey, thus achieving a global search; When $|\boldsymbol{B}|\leq 1$, the gray wolf will focus on searching a certain area, so as to realize local search.

Prediction model of ppv underwater blasting based on gwo-svr

The collected blast vibration data is first divided into a test data set and a training data set, 20% of these data are taken as test data, and the remaining 80% are training data sets. The initialisation parameters of the GWO algorithm are then set, namely the maximum number of iterations, and the number of individuals in the wolf pack, both set to 20 this time. In addition, according to the penalty parameter c and kernel function parameter g that need to be selected by the SVR machine, the range of these two optimization parameters is set. This time, the value range of these two parameters is set to 0.01~100.

The fitness function is an index that describes the performance of parameters, and is an evaluation criterion to determine whether the current target parameter value is optimal. The mean square error (*MSE*) is the expected value of the square of the difference between the predicted data and the test data. When the *MSE* is the minimum value, it is considered that the target parameter value reaches the optimal standard. This time the mean squared deviation was chosen as the fitness function.

Finally, the GWO-SVR model is trained with the training data set. When the *MSE* takes the minimum value, the model is optimal, and the parameters obtained at this time are the optimal parameters. The GWO-SVR model is then tested with test data to assess the performance of the model. The specific process is shown in Figure 3.

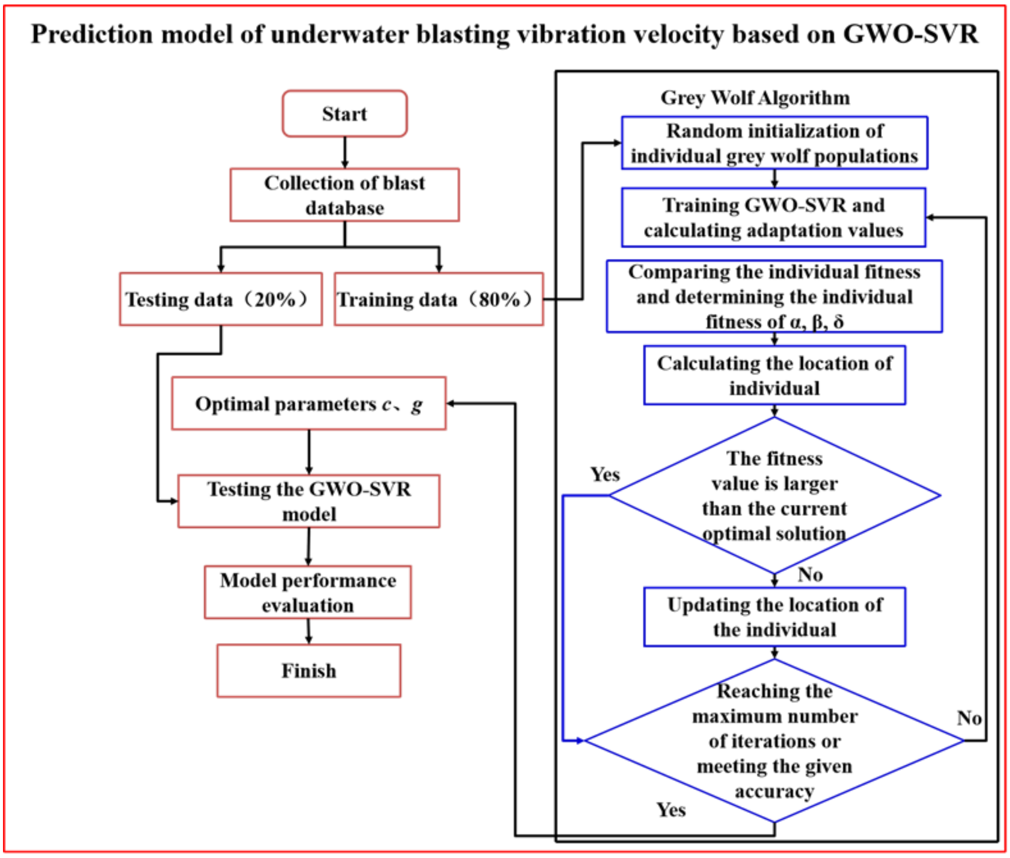

Figure 3. Prediction model of underwater blasting vibration velocity based on GWO-SVR

Analysis of prediction results

The prediction model of underwater blasting vibration velocity needs to be evaluated according to the discreteness and correctness of the predicted data. In this paper, the prediction results obtained by the double-layer neural network, the medium decision tree, and the empirical SVR model are compared with the prediction results of GWO-SVR, and the actual value-prediction value graph and residual comparison, as well as regression evaluation indicator are used to evaluate the performance of the model. The four models have the hole length (HL), spacing (S), row spacing (R_s), burden (B), stemming length (l_s), the distance of blasting center (B_d), height differential elevation (H_{de}), seawater pressure (P_s), powder factor (PF), maximum charge of single hole (Q_{smax}), maximum charge per delay (Q_{max}) and total charge (Q_{tot}) are used as model inputs, and the PPV is used as output. The models are first trained with nearly 80% (24) of the datasets, then the models are tested with the remaining 20% (6) of the datasets, and finally the prediction results of the 4 models are evaluated.

The parameters of each model are set as follows: the size of the first layer of the double-layer neural network model is 10, the size of the second layer is 10, the neuron activation function is ReLU, and the iteration limit is 1000; The minimum leaf size of the medium decision tree is 12; the kernel function of the empirical SVR model is the RBF kernel function, c is 100, and g is 1; The kernel function of the GWO-SVR model is the RBF kernel function. The optimal c obtained by optimizing the parameters of SVR based on GWO is 0.010219, and the optimal g is 98.5121.

Comparison of actual-predicted value plots and residuals

The actual-predicted value plot reflects the abnormity due to random effects and provides a visual assessment of model fit. The comparison chart of blasting vibration velocity prediction results and actual distance is shown in Figure 4. From the view of No. 6 in Figure 4, the blue column deviates greatly from the red column, indicating that the PPV predicted by the double-layer neural network has a large deviation from the actual situation; As can be seen from No. 4 in Figure 4 , the green column deviates significantly compared to the red column, indicating that the PPV predicted by the medium decision tree model has a large deviation from the actual situation; On the whole, the purple and yellow columns fluctuate correspondingly with the changes of the red column, and the deviation is small, indicating that the PPV predicted by the GWO-SVR model and the empirical SVR model has a small deviation from the actual situation.

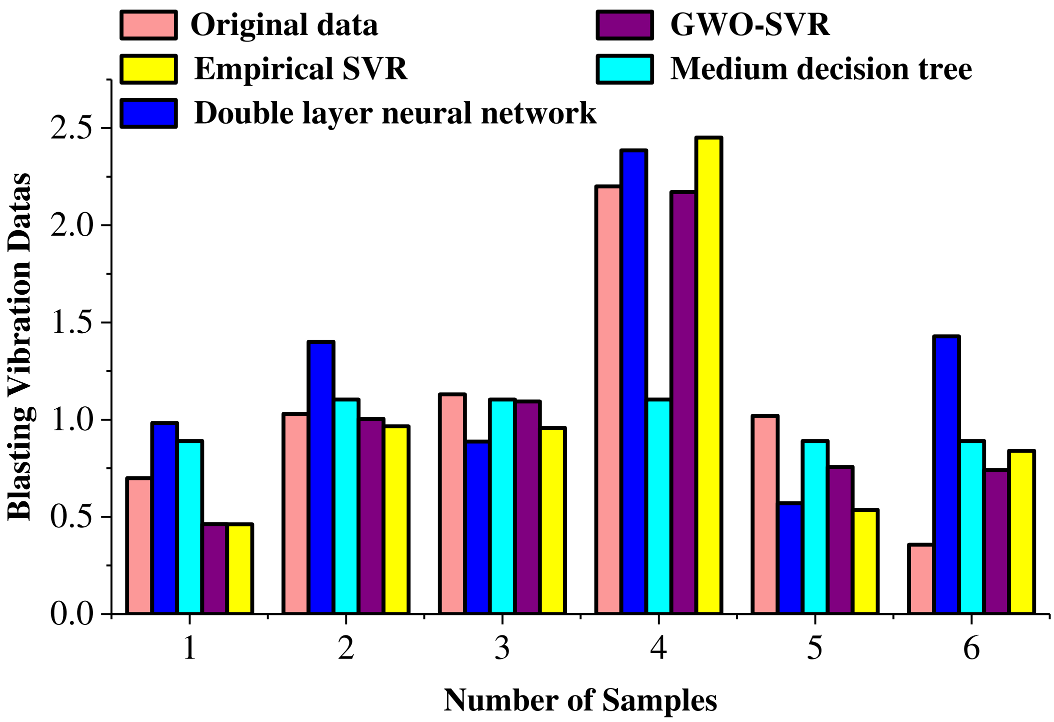

Figure 4. Comparison of predicted PPV results from different models with the actual situation

Residual in mathematical statistics refers to the difference between the actual observed value and the predicted value, which can intuitively reflect the deviation between the predicted data and the real data. In order to analyze the deviation of the actual PPV from the predicted PPV in detail, the residuals of different models are calculated and the corresponding graphs are drawn, as shown in Figure 5. As can be seen from No. 6 in Figure 5, the absolute value of the residual error predicted by the double-layer neural network is very large, and the maximum value of the residual error reaches -1.1

cm/s; and the absolute value of the residuals predicted by the medium decision tree is also large, with the maximum value of the residuals reaching 1.1 cm/s, as can be seen from the ordinal No 4 in Figure 5. Thus, it is shown that double-layer neural networks and medium decision trees are less effective in prediction.

It can be determined from Figure 4 and Figure 5 that the double-layer neural network model and the medium decision tree model have the worst data prediction effect, and the performance of the other two models can't be judged.

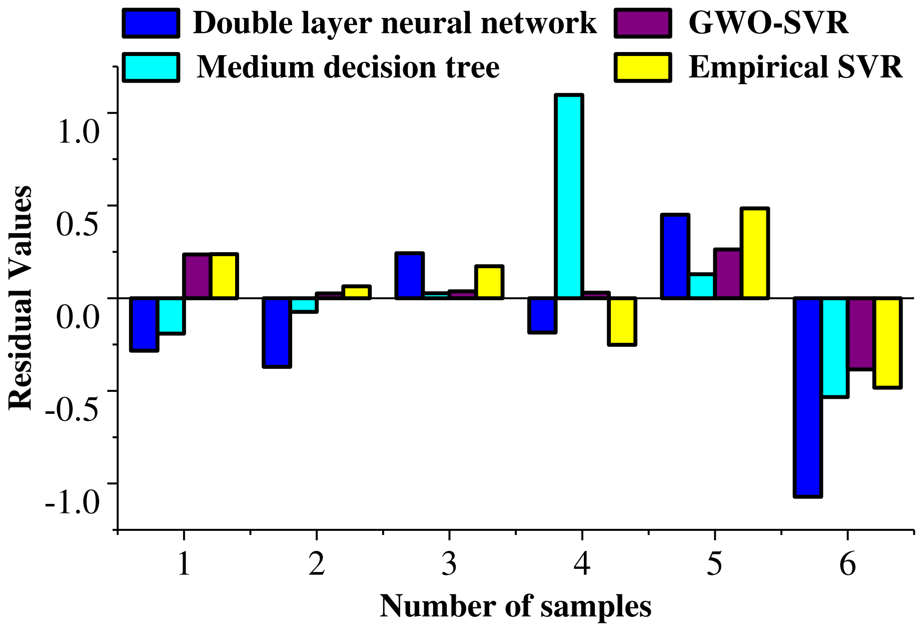

Figure 5. Plot of residuals of PPV results predicted by different models

Comparison of regression evaluation indicators

The commonly used prediction model regression evaluation indicators include R-square, root mean square error, mean square error and mean absolute error. Therefore, this section uses these four indicators to evaluate the effect of the prediction model. R-squared (R^2) is a statistical indicator used to reflect the closeness of the correlation between variables, as shown in equation (11). The root mean square error (*RMSE*) is the square root of the ratio of the sum of the squares of the deviations of the observations from the true value to the number of observations in statistics, as shown in equation (12); The mean squared error (*MSE*) is the sum of the squares of the absolute errors and then averaged, as shown in equation (13); The mean absolute error (*MAE*) is the average of the absolute errors, as shown in Equation (14). When R^2=1, *RMSE*=0, *MSE*=0 and *MAE*=0, it means that the predicted value of the model matches perfectly with the true value.

$$R^2 = \frac{(n\sum X_{obs}X_{model} - \sum X_{obs}X_{model})^2}{(n\sum X_{obs}^2 - (\sum X_{obs})^2)(n\sum X_{model}^2 - (\sum X_{model})^2)} \qquad (14)$$

$$RMSE = \sqrt{\frac{1}{M}\sum_{i=1}^{m}(X_{obs,i} - X_{model,i})^2} \tag{15}$$

$$MSE = \frac{1}{n}\sum_{i=1}^{n}(X_{obs,i} - X_{model,i})^2 \tag{16}$$

$$MAE = \frac{1}{m}\sum_{i=1}^{m}\left|X_{obs,i} - X_{model,i}\right| \tag{17}$$

The prediction results of the four models are evaluated using regression evaluation indicators, and the regression evaluation indicators are shown in Table 2.

Table 2. The regression evaluation index of different flying rocks prediction models

Types of predictive models	R^2	*RMSE*	*MSE*	*MAE*
Double layer neural network	0.14	0.52616	0.27685	0.43393
Medium decision tree	0.20	0.50764	0.2577	0.34181
GWO-SVR	0.9285	0.21424	0.0459	0.1625
Empirical SVR model	0.8762	0.32171	0.1035	0.282

As can be seen from the Table 2, the prediction model of underwater blasting vibration velocity based on double-layer neural network has the smallest R^2 (0.14), the largest *RMSE* (0.52616), *MSE* (0.27685) and *MAE* (0.43393) values; The medium decision tree prediction model has R^2 of 0.20, *RMSE* of 0.50764, *MSE* of 0.2577, and *MAE* of 0.34181; The empirical SVR prediction model has R^2 of 0.8762, *RMSE* of 0.32171, *MSE* of 0.1035, and *MAE* of 0.282. This model and the medium decision tree prediction model have general regression evaluation indicators; The GWO-SVR prediction model has the largest R^2 (0.9285), the smallest *RMSE* (0.32171), *MSE* (0.1035) and *MAE* (0.282) values. Comparing the GWO-SVR prediction model with the empirical SVR prediction model, it's found that R^2 is increased by 0.0523, *RMSE* is decreased by 0.10747, *MSE* is decreased by 0.0576, and *MAE* is decreased by 0.1195. Therefore, it can be seen from the regression evaluation indexes of each prediction model that the prediction model of underwater blasting vibration velocity established based on GWO-SVR is the best.

Conclusion

The assessment of the safety of buildings is a major problem faced by the safety production of underwater blasting. Predicting the PPV of blasting is one of the effective ways to alleviate this problem. In order to further improve the prediction accuracy of blasting PPV, the GWO algorithm is used to iteratively optimize the penalty factor and radial basis kernel function parameters of the SVR model, and a prediction model of blasting PPV is established. Based on the engineering background of the Dajin Island water intake open channel of Guangdong Taishan Nuclear Power Plant Phase 1 Project, the comparison and analysis of the predicted value of the model with the prediction results of the double-layer neural network, medium decision tree and empirical SVR model, it is proved that the

GWO-SVR model has the best prediction effect, the conclusions are as follows:

(1) Taking the Dajin Island water intake open channel of the first phase of Guangdong Taishan Nuclear Power Station as the engineering background, the establishment of hole length (*HL*), spacing (*S*), row spacing (R_s), burden (*B*), stemming length (l_s), the distance of blasting center (B_d), height differential elevation (H_{de}), seawater pressure (P_s), powder factor (*PF*), maximum charge of single hole (Q_{smax}), maximum charge per delay (Q_{max}) and total charge (Q_{tot}) are used as model inputs, and the PPV is used as the output database.

(2) The parameters *c* and *g* of the SVR model are optimised by the GWO algorithm, and the GWO algorithm is combined with the SVR algorithm to build a blast PPV prediction model, and the prediction results of this model are compared with those of the medium decision tree model, the double-layer neural network model and the empirical SVR model.

(3) The actual value-predicted value plot and residual analysis show that the prediction model of PPV based on double-layer neural network has the worst prediction effect, and the performance of the other three models can't be judged yet.

(4) Through the comparison and analysis of regression evaluation indicators, the prediction effect of the PPV prediction model established based on GWO-SVR is the best, and its R^2 value is 0.9285, *RMSE* value is 0.21424, *MSE* value is 0.0459, and *MAE* value is 0.1625.

(5) Based on the analysis of (3) and (4), it is concluded that the prediction model of blasting PPV based on GWO-SVR is the best.

Funding This research was funded by the Launching project of high-level talents of Jiangxi University of Science and Technology (205200100486) and Science and technology project of Jiangxi Provincial Department of Education (GJJ200871) and Youth Projects of Guangdong Education Department for Foundation Research and Applied Research (6021210080k).

Declaration

Conflict of interest The authors declare that there is no confict of in terest.

Acknowledgement

This research was funded by the Launching project of high-level talents of Jiangxi University of Science and Technology (205200100486) and Science and technology project of Jiangxi Provincial Department of Education (GJJ200871) and Youth Projects of Guangdong Education Department for Foundation Research and Applied Research (6021210080k).

References

[1] Verma, H. K., Samadhiya, N. K., Singh, M., Goel, R. K., & Singh, P. K. (2018). Blast induced rock mass damage around tunnels. Tunn. Undergr. Space Technol, *71*, 149–158. [CrossRef]

[2] Zhang, X., Nguyen, H., Bui, X. N., Tran, Q. H., Nguyen, D. A., & Bui, D. J. (2019). Novel soft computing model for predicting blast-induced ground vibration in open-pit mines based on particle swarm optimization and XGBoost. Natural Resources Research. https://doi.org/10.1007/s11053-019-09492-7.

[3] Li, X. F., Li, H. B., & Zhang, G. K. (2019). Damage assessment and blast vibrations controlling considering rock properties of underwater blasting. International Journal of Rock Mechanics and Mining Sciences, 121, 104045.

[4] Wang, Z. X., Gu, W. B., Liang, T., Zhao, S. T., Chen, P., & Yu, L. F. (2020). Monitoring and Prediction of the Vibration Intensity of Seismic Waves Induced in Underwater Rock by Underwater Drilling and Blasting. Defence Technology.

[5] Lu, W., Yang, J., Chen, M., & Zhou, C. (2011). An equivalent method for blasting vibration simulation. Simulation Modelling Practice and Theory, 19(9), 2050-2062.

[6] Zhang, Z., Gao, W., Li, K., & Li, B. (2020). Numerical simulation of rock mass blasting using particle flow code and particle expansion loading algorithm. Simulation Modelling Practice and Theory, 104, 102119.

[7] Duvall, W. I., & Fogelson, D. E. (1962). Review of criteria for estimating damage to residences from blasting vibrations (Vol. 5968). US Department of the Interior, Bureau of Mines..

[8] Zhang, W., Ma, N., Ren, J., & Li, C. (2021). Peak particle velocity of vibration events in underground coal mine and their caused stress increment. Measurement, 169, 108520.

[9] Wang, X., & Cai, M. (2017). Numerical modeling of seismic wave propagation and ground motion in underground mines. Tunnelling and underground space technology, 68, 211-230.

[10] Hao, H., Wu, C., & Zhou, Y. (2002). Numerical analysis of blast-induced stress waves in a rock mass with anisotropic continuum damage models part 1: equivalent material property approach. Rock Mechanics and Rock Engineering, 35(2), 79–94.

[11] Saiang, D., & Nordlund, E. (2009). Numerical analyses of the influence of blast-induced damaged rock around shallow tunnels in brittle rock. Rock Mechanics and Rock Engineering, 42, 421–448.

[12] Wang, Y., Wen, Z., Liu, G., Wang, J., Bao, Z., Lu, K., & Wang, B. (2020). Explosion propagation and characteristics of rock damage in decoupled charge blasting based on computed tomography scanning. International Journal of Rock Mechanics and Mining Sciences, 136, 104540.

[13] Nguyen, H., Drebenstedt, C., Bui, X. N., & Bui, D. T. (2019). Prediction of blast-induced ground vibration in an open-pit mine by a novel hybrid model based on clustering and artificial neural network. Natural Resources Research. https://doi. org/10.1007/s11053-019-09470-z.

[14] Shang, Y., Nguyen, H., Bui, X. N., Tran, Q. H., & Moayedi, H. (2019). A novel artificial intelligence approach to predict blast-induced ground vibration in open-pit mines based on the firefly algorithm and artificial neural network. Natural Resources Research. https://doi.org/10.1007/s11053-019-09503-7.

[15] Taheri, K., Hasanipanah, M., Bagheri Golzar, S., & Abd Majid, M. Z. (2017). A hybrid artificial bee colony algorithm-artificial neural network for forecasting the blast-produced ground vibration. Engineering with Computers, 33, 689-700.

[16] Yang, H., Hasanipanah, M., Tahir, M. M., & Bui, D. T. (2019). Intelligent prediction of blasting-induced

ground vibration using ANFIS optimized by GA and PSO. *Natural Resources Research.* https://doi.org/10.1007/s11053-019-09515-3.

[17] Khandelwal, M., Armaghani, D. J., Faradonbeh, R. S., Yellishetty, M., Abd Majid, M. Z., & Monjezi M. (2017). Classification and regression tree technique in estimating peak particle velocity caused by blasting. Engineering with computers, 33(1), 45-53.

[18] Rana, A., Bhagat, N. K., Jadaun, G. P., Anindya Pain, S. R., & Singh, P. K. (2020). Predicting blast-induced ground vibrations in some Indian tunnels: a comparison of decision tree, artificial neural network and multivariate regression methods. Mining, Metallurgy & Exploration, 37(4), 1039-1053.

[19] Bhagat, N. K., Mishra, A. K., Singh, R. K., Sawmliana, C., & Singh, P. K. (2022). Application of logistic regression, CART and random forest techniques in prediction of blast-induced slope failure during reconstruction of railway rock-cut slopes. Engineering Failure Analysis, 106230.

[20] Hasanipanah, M., Monjezi, M., Shahnazar, A., Armaghani, D. J., Farazmand, A. (2015). Feasibility of indirect detennination of blast induced ground vibration based on support vector machine. Measurement, 75, 289-297.

[21] Khandelwal, M. (2011). Blast-induced ground vibration prediction using support vector machine. Engineering with Computers, 27(3), 193-200.

[22] Shi, X., Zhou, J., & Li, X. (2012). Utilization of a nonlinear support vector machine to predict blasting vibration characteristic parameters in opencast mine. Przeglad Elektrotechniczny, 88(9b), 127-132.

[23] Yang, H., Rad, H. N., Hasanipanah, M., Amnieh, H. B., & Nekouie, A. (2019). Prediction of Vibration Velocity Generated in Mine Blasting Using Support Vector Regression Improved by Optimization Algorithms. Natural Resources Research, 29(2), 807-830.

[24] Paneiro, G., Durão, F. O., e Silva, M. C., & Falcão Neves, P. (2018). Artificial neural network model for ground vibration amplitudes prediction due to light railway traffic in urban areas. Neural Computing and Applications, 29(11), 1045-1057.

[25] Lawal, A. I., & Idris, M. A. (2020). An artificial neural network-based mathematical model for the prediction of blast-induced ground vibrations. International Journal of Environmental Studies, 77(2), 318-334.

[26] Hasanipanah, M., Faradonbeh, R. S., Amnieh, H. B., Armaghani, D. J., & Monjezi, M. (2017). Forecasting blast-induced ground vibration developing a CART model. Engineering with Computers, 33(2), 307-316.

[27] Nguyen, H., Bui, X. N., Bui, H. B., & Cuong, D. T. (2019). Developing an XGBoost model to predict blast-induced peak particle velocity in an open-pit mine: a case study. Acta Geophysica, 67(2), 477-490.

[28] Abdi, M. J., & Giveki, D. (2013). Automatic detection of erythemato-squamous diseases using PSO-SVM based on association rules. Engineering Applications of Artificia Intelligence, 26(1), 603-608.

[29] Hasanipanah, M., Shahnazar, A., Amnieh, H. B., & Armaghani, D. J. (2017). Prediction of air-overpressure caused by mine blasting using a new hybrid PSO-SVR model. Engineering with Computers, 33(1), 23-31.

[30] Armaghani, D. J., Koopialipoor, M., Bahri, M., Hasanipanah, M., & Tahir, M. M. (2020). A SVR-GWO technique to minimize flyrock distance resulting from blasting. Bulletin of Engineering Geology and the Environment, 79(8), 4369-4385.

[31] Murillo-Escobar, J., Sepulveda-Suescun, J. P., Correa, M. A., & Orrego-Metaute, D. (2019). Forecasting concentrations of air pollutants using support vector regression improved with particle swarm optimization: Case study in Aburra Valley, Colombia. Urban Climate, 29, 100473.

[32] Khandelwal, M., & Singh, T. N. (2009). Prediction of blast induced ground vibration using artificial neural network. International Journal of Rock Mechanics and Mining Sciences, 46(7), 1214–1222.

[33] Khandelwal, M. (2011). Blast-induced ground vibration prediction using support vector machine. Engineering with Computers, 27(3), 193–200.

[34] Hajihassani, M., Jahed Armaghani, D., Marto, A., & Mohamad, E. T. (2015a). Ground vibration prediction in quarry blasting through an artificial neural network optimized by imperialist competitive algorithm. Bulletin of Engineering Geology and the Environment, 74(3), 873–886.

[35] Hajihassani, M., Jahed Armaghani, D., Monjezi, M., Mohamad, E. T., & Marto, A. (2015b). Blast-induced air and ground vibration prediction: A particle swarm optimization-based artificial neural network approach. Environmental Earth Sciences, 74(4), 2799–2817.

[36] Balogun, A. L., Rezaie, F., Pham, Q. B., Gigović, L., Drobnjak, S., Aina, Y. A., & Lee, S. (2021). Spatial prediction of landslide susceptibility in western Serbia using hybrid support vector regression (SVR) with GWO, BAT and COA algorithms. Geoscience Frontiers, 12(3), 101104.

[37] Zeng, Y. Q.，Wang, C. B.，& Zhao, H. L. (2016). Monitoring and analysis of blasting vibration of open channel in Taishan Nuclear Power Station. Journal of Anhui University of Science and Technology (Natural Science), 36(2), 68-75.

[38] Liu, Y. Q., Li, H. B., Pei, Q. T., & Zhang, W. (2013). Prediction of peak particle velocity induced by underwater blasting based on the combination of grey relational analysis and genetic neural network[J]. Rock and Soil Mechanics, 34(1): 259-264.

[39] Smola, A. J., & Schölkopf, B. A. (2004). Tutorial on support vector regression. Statistics and computing, 14(3): 199-222.

[40] Mahmoodzadeh, A., Mohammadi, M., Noori, K. M. G., Khishe, M., Ibrahim, H. H., Ali, H. F. H., & Abdulhamid, S. N. (2021). Presenting the best prediction model of water inflow into drill and blast tunnels among several machine learning techniques. Automation in Construction, 127, 103719.

[41] Cortes, C., & Vapnik, V. (1995). Support-vector networks. Mach Learn, 20(3), 273–297.

[42] Emary, E., Zawbaa, H. M., & Hassanien, A. E. (2016). Binary grey wolf optimization approaches for feature selection. Neurocomputing, 172, 371-381.

[43] Mirjalili, S., Mirjalili, S. M., & Lewis, A. (2014). Grey wolf optimizer. Advances in engineering software, 69, 46-61.